Journal of Advances and Scholarly Researches in Allied Education
Vol. 16, Issue No. 2, February-2019, ISSN 2230-7540

Crystal Structure & Morphology, Band Gap Energy, Photoluminescence and Dye Degradation of X-Ray Diffraction Spectrum

Pooja*

Extension Lecturer of Chemistry, Govt. College, Israna, Panipat

Abstract – Developing nations need to propel their financial development by expanded modern action because of their expansion in populace. Such businesses are the major reason for water contamination. Ventures, for example, the textile industry produce organic dyes and these dyes can never again be expelled by biodegradable methods without trouble. Such dyes can be poisonous to oceanic creatures, plants and the human body. Zr doped ZnO nanoparticles are set up by the sol-gel method with post-annealing. thin films of Zr-doped ZnO, with Zr concentrations fluctuating from 0 to 5 at%, have been readied utilizing a sol-gel method. Crystallinity, microstructure, and optical properties influenced by Zr concentration were explored. Doped ZnO with Zr has been gotten by sol-gel method and portrayed by powder X-ray diffraction, energy dispersive X-ray spectrum, Scanning electron micrographs, and UV–visible diffuse reflectance and photoluminescence spectroscopy. Powder XRD demonstrates that synthesized Zr doped ZnO has hexagonal wurtzite structure and high crystallinity, DRS uncovers that wavelength are shifted from UV district to visible locale when Zr doping. PL spectra obviously uncover that the recombinations of electron-hole pair in ZnO are stifled by Zr doping. Zr-doping improves the photocatalytic debasement of methylene blue dye than ZnO under visible light. The impact of Zr substance on the structure, morphology, absorption, emission, and photocatalytic action of ZnO SNPs was examined efficiently.

Keywords: Doped, Photocatalytic, Sol-gel Method, Zr-ZnO, Visible Light, Methylene Blue Dye, diffraction spectrum, crystal size, surface area

----------X----------

1. INTRODUCTION

Lately, numerous analysts are found the new and altered semiconductor materials and use of these materials is cleaning the dangerous effluents. ZnO photocatalyst is 3.2 eV and high photoactivity in UV spectrum. ZnO photocatalyst are utilized in luminescence, optics, optoelectronics, sensors, actuators, energy, biomedical sciences, and spintronics. ZnO has been utilized as a photocatalyst, inferable from its high action, minimal effort and friendly environment. Nonetheless, the issue of ZnO is the high recombination rate of electron-hole pair, bringing about low degradation efficiencies of the organic contaminations. To beat these restrictions, various methodologies have been received to improve the charge separation effectiveness and afterward upgrade the photocatalytic action of the impetus, for example, the Semiconductors doping or hybridizing. ZnO adjusted with FeO semiconductor. To think about the impacts of Zr-doped ZnO and nanosized ZrO2 framework structure and photocatalytic performance and ultrasoft pseudopotential method additionally impact ZnO structure. Impact of Zr doping andZr-Al co doping on the electrical and optical properties of ZnO. Report that the grain size of Zr-doped ZnO is little and the surface area is high. Additionally, within 0.2-1at% Zr-doping, the higher the doping amount is, the more grounded the photocatalytic action. Used sol-gel method to think about the impacts of Zr-doping on ZnO photoelectric properties. The outcomes demonstrated that when Zr-doping fell in 0-5at%, the protections of all the doping frameworks all were more noteworthy than that of pure ZnO. Also, when the doping amount was 3at%, the transmissivity of the doping framework was the best. Kim et al. to ponder the photoelectric property of Zr-doped ZnO framework by utilizing beat laser deposition method. The outcomes show that the higher the oxygen weight is, the more prominent the doping framework obstruction is and the higher the transmissivity. Numerous methods are accounted for as synthesize coupled metal oxides are photograph deposition method solid state scattering method aqueous method impregnation method, sol– gel method, co-precipitation method mechanical

blending method, fire spray pyrolysis and microwave synthesis.

Doped zinc oxide is of enthusiasm as a transparent conductive oxide (TCO), because of its low resistivity (ď10'$_3$ Ω¨ cm), high transparency (>80%) and wide bandgap (3.37 eV). The bounty, and subsequently ease of the real constituents, makes this an alluring option in contrast to indium tin oxide (ITO), which contains generally rare and costly indium. TCOs must have low resistivity (ď10'$_3$ Ω¨ cm), high transparency (>80% in the visible range) and high bearer concentration (ě1020 cm'$_3$). ZnO will in general be characteristically n-type and can be promptly doped to degeneracy, subsequently giving high conductivity. The high transporter thickness coming about because of the ruffian doping could likewise instigate optical gap increments because of band filling impacts (i.e., Burstein-Moss impact), which upgrades transparency in the short wavelength district. The dopants utilized in ZnO ought to be shallow donors that give additional ionized electrons. Dopants, for example, B, In, Co, Zr, Ge, Hf, Sn have been considered, while the most well-known dopants are Al and Ga. The announced electrical and optical properties for doped ZnO are being improved by utilizing distinctive dopants so as to rival ITO, which has a resistivity in the order of 10'4 Ω¨ cm and transparency ě85%.

The present paper reports the environmentally friendly greener synthesis of novel Zr-doped ZnO utilizing sol-gel synthesis and examinations on its photocatalytic movement under visible light for the degradation of MB dye.

2. REVIEW OF LITERATURE

M. C. Uribe López, (2019) - ZnO-ZrO_2 nanocomposites utilizing zinc (II) acetylacetonate and distinctive ZnO substance (13, 25, 50, and 75% mol) were synthesized through sol-gel method. The synthesis procedure was firmly identified with nanocomposite properties particularly on their structural composition. The got ZnO-ZrO2 nanomaterials introduced tetragonal crystalline structure for zirconia though hexagonal one was framed in ZnO. Raman spectroscopy and XRD designs affirmed the development of tetragonal zirconia while restraint of monoclinic structure was watched. Expansion of ZnO influenced the pore size distribution of the composite, and the deliberate explicit surface areas were from 10 m2/g (for pure ZnO) to 46 m2/g (perfect ZrO_2). Eg estimations of ZrO_2 were changed by ZnO expansion, since determined qualities utilizing Kubelka-Munk's capacity fluctuated from 4.73 to 3.76 eV. The morphology and size of the nanomaterials researched by electron microscopy demonstrated arrangement of nanorods for ZnO with sizes extending from 50 nm to 300 nm while zirconia was framed by littler particles (under 50 nm). The fundamental favorable position of utilizing the nanocomposite for photocatalytic degradation of phenol was the mineralization degree, since 75ZnO-ZrO_2 nanocomposite outperformed mineralization come to by pure ZnO and furthermore hindered development of unwanted intermediates.

Parangusan H (2018) - Pure ZnO and Yttrium-doped (Y-doped) ZnO at different mol% with flower-like nanostructures are synthesized by a microwave-assisted sol-gel method, trailed by exploring the morphologies, crystal structures, optical properties and photocatalytic performances. While the stage developments are distinguished by X-ray diffraction strategy, both examining and transmission electron microscopy pictures unmistakably portray the flower-like morphology of ZnO and Y-doped ZnO samples. Arrangement of flower petals is from the nanoparticles that developed and associated by introduction connection process. The flower-like architecture is tended to regarding an Ostwald aging system. The UV-Vis absorption considers show improved absorption for the Y-doped ZnO, while the photoluminescence spectra affirm the essentialness of sample defects in the photocatalytic degradation of organic toxins. Impacts of different experimental parameters, for example, the amount of photocatalysts, dye concentration and dopant concentration on the dye degradation are likewise upgraded.

Jun Song, (2017) - Self-standing photocatalytic layers built from TiO_2nanofibers hold extraordinary guarantee in natural remediation; in any case, challenges still stayed for the poor mechanical properties of polycrystalline TiO_2 nanofibers. Thus, delicate Zr-doped TiO_2 (TZ) nanofibrous membranes with strong mechanical properties and upgraded photocatalytic movement were fabricated through electrospinning strategy. The Zr4+ fuse could adequately repress the grain development and decrease the surface deformities and limit of TiO2nanofiber. The as-arranged TZ layers were made out of well-interconnected nanofibers with a high viewpoint proportion, little grain size and pore size, which displayed great rigidity (1.32 MPa) and demonstrated no conspicuous harm after 200 cycles of twisting to a sweep of 2 mm. A conceivable bowing twisting system of the delicate TZ layers was proposed from tiny single nanofiber to macro-scopical layers. Additionally, the resultant TZ layers showed better photocatalytic performance for methylene blue degradation contrasted with a business catalyst (P25), including high degradation level of 95.4% within 30 min, great reusability in 5 cycles, and effortlessness of reusing. The effective planning of such intriguing materials may open up new avenues for the structure and advancement of soft TiO2-based layers for different application.

Lin et al. (2011) - announced an examination on Zr doped ZnO films stored by ALD, covering points, for example, the conductivity improvement and

bandgap increment in the wake of doping, while at the same time concentrating on the impact of annealing the doped samples. The present examination develops on this examination by investigating how the Zr doping consolidated in the cross section, distinguishes conceivable reasons for the carrier density decline at high doping, explores the doping impact on the grain development, lastly looks at the purpose behind the optical gap increment after of doping.

Kapusuz et al., (2013) - effectively synthesized composites by doping and co-doping B and Zr particles in anatase TiO2 lattice by utilizing sol-gel method to demonstrate expanded photocatalytic performance to larger amounts. It was inferred that photocatalytic activity of TiO_2 expanded by doping with B and Zr which result in formation of oxygen opening in crystal and furthermore forming Ti4+ absconds which result in formation of more energy levels and in this way increment the photocatalytic activity.

3. EXPERIMENTAL SETUP AND MATERIAL& METHODS

- ***Materials***

$Zr(NO_3)_3$(Loba-chemi), $Zn(NO_3)_2$(Loba-chemi), Methylene blue dye(Merck) and liquid ammonia(Qualigens) were utilized. Distilled water is utilized for the makeup solution.

- ***Methods***

√ **Preparation of Zr-ZnO by Sol-gel method**

To appropriate concentration of Zn $(NO_3)_2$ and Zr $(NO_3)_3$ solution was included under stirring. After 1:1 fluid ammonia solution was added to achieve a pH 9.5 under constant stirring. The crystals were gathered by filtration, dried and calcined at 500°C for 1 h in a suppress heater fitted with a PID temperature controller. The warming rate was 10°C min^{-1}. The undoped ZnO crystals were synthesized by receiving a similar system however without $Zr(NO_3)_3$. The chemicals utilized were of logical evaluation and deionized distilled water was utilized for the investigations.

- ***Characterization Techniques***

A PANalyticalX'Pert PRO diffractometer with Cu Ka rays of 1.5406 Å was utilized to record the powder X-ray diffractograms (XRD) of the samples at 40 kV and 30 mA with a scan rate of 0.04°s^{-1} of every a 2θ scope of 10– 75°. The morphologies of Zr-doped ZnO and ZnO synthesized by sol-gel method were evaluated utilizing a JSM6610 model scanning electron microscope (SEM) under vacuum mode. The energy dispersive X-ray (EDX) spectrum was gotten utilizing the Oxford instruments joined to scanning electron microscope (SEM). The diffuse reflectance spectra were acquired with a PerkinElmer Lamda 35 spectrometer. A PerkinElmer LS 55 fluorescence spectrometer was utilized to record the photoluminescence (PL) spectra at room temperature.

- ***Photocatalytic Activity***

The visible light photocatalytic thinks about were made in an immersion type photo reactor outfitted with a 150-W tungsten halogen lamp fitted into a twofold walled borosilicate immersion well of 40 mm external width with channel and outlet for dissemination of $K_2Cr_2O_7$ solution. The 1N K2Cr2O7 solution utilized evacuates 99 % of the UV light with wavelength somewhere in the range of 320 and 400 nm and goes about as an UV cutoff channel. After the expansion of the catalyst to the dye solution, air was risen through the solution which held the catalyst particles under suspension and at constant motion. The catalyst was isolated after the brightening. The dye Methylene blue was dissected spectrophotometrically at 656 nm.

4. DATA ANALYSIS AND RESULT

■ ***Crystal Structure and Morphology***

The energy dispersive X-ray diffraction spectrum of Zr-ZnO is appeared in figure 1. It is uncovering that Zr, Zn and O component. It is reasoning that 1.83% Zr doped ZnO lattice. Figure 2. Demonstrates that the scanning electron microscope picture of Zr-ZnO particles. It is demonstrating that hexagonal structures of ZnO are demolished with doped Zr^{3+} particle. It is additionally affirming that doped ZnO as micron size.

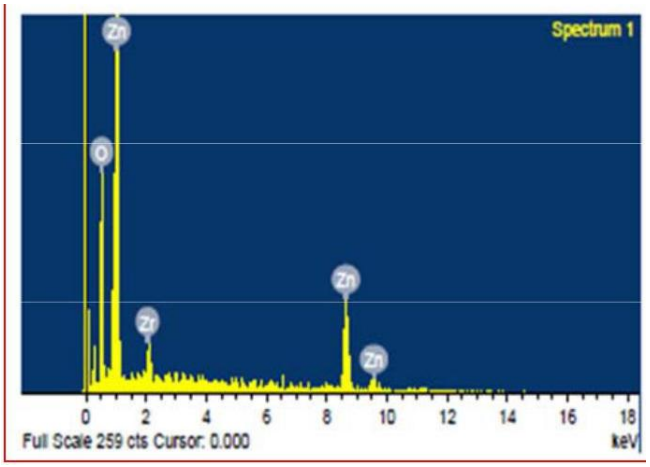

Figure 1. X-ray spectrum of Zr-ZnO

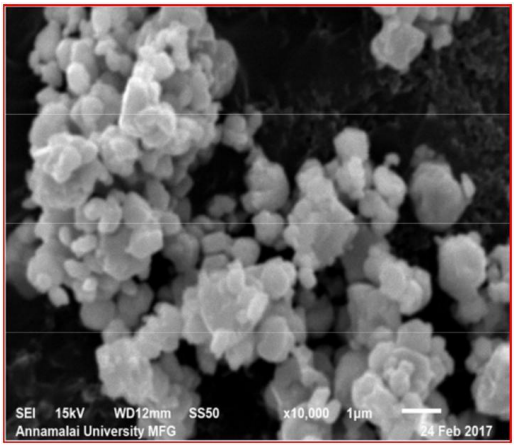

Figure 2. Scanning Electron Microscope of Zr-ZnO.

The powder X-ray diffraction spectra of ZnO and Zr-ZnO are appeared in figure 3. For exposed ZnO, the diffraction peaks are situated at 2θ=31.737, 34.379, 36.215, 47.484, 56.536, 62.777, 66.304, 67.868, and 69.009 are related with planes separately. This example has been ordered as hexagonal wurtzite period of ZnO with lattice constants a=b=0.324nm and c=0.521 nm (JPCDS card number: 89-1397), and further it is additionally affirmed that the synthesized catalyst is free of contaminations as it doesn't contain any trademark XRD peaks other than ZnO peaks. Sol-gel synthesized Zr-ZnO diffraction design absolutely coordinate with uncovered ZnO design. Further, the nonappearance of cubic period of ZrO_2 peak at 2θ esteem is 30.30, 35.40, 50.60, 59.8, 62.85° (JCPDS card no: 27-0997), monoclinic (JCPDS no 37-1484) and tetragonal phase (JCPDS no: 86-0965) of ZrO2 are missing in Zr-ZnO catalyst. Sharp diffraction peaks show that the samples have high crystallinity. The average particle size (D) is determined by utilizing the Debye-Scherrer's condition $D = 0.9\lambda/\beta\cos\theta$. Where, λ is the X-ray wavelength of 1.54 Å, β is the full-width at half most extreme, θ is the Bragg's diffraction edge and surface area determined by S = 6/ρD, where S is the particular surface area, D is the average particle size and ρ is the material density. From the table-1, the crystal size of exposed ZnO and Zr-ZnO are 10.06 and 12.16 nm relating surface area is 105.2 and 73.08m^2g^{-1} separately. It is likewise demonstrating that the average particles size no change with Zr doped contrast with exposed ZnO.

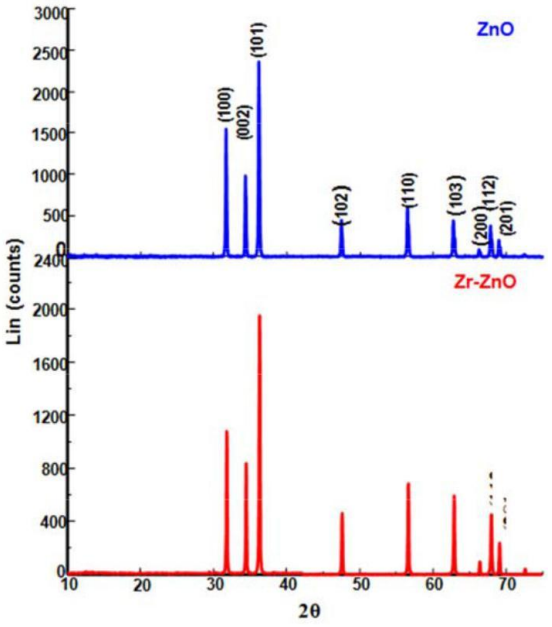

Figure 3. X-ray diffraction spectrum

Table 1. Crystal size (D) and Surface area (S)

Oxide	*D*, nm	*S*, m^2g^{-1}
ZnO	10.08	105.2
Zr-ZnO	12.16	73.08

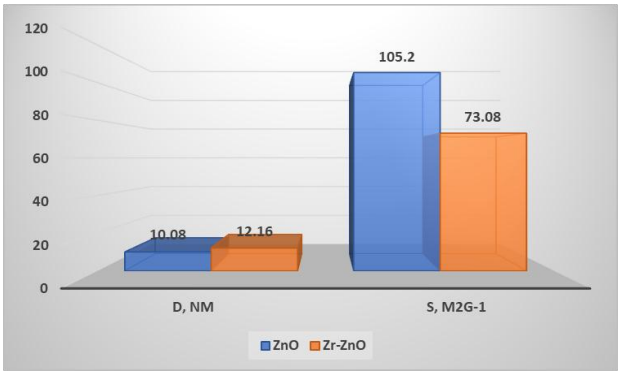

Figure 4. Crystal size (D) and Surface area (S)

■ ***Band Gap Energy***

The diffuse reflectance spectrum of Zr-ZnO are appeared in figure 5. In Zr-ZnO particles has higher absorption in visible area contrast with exposed ZnO (not appeared in figure). To figure the band gap energies of Zr-ZnO catalysts, UV– vis spectra in the diffuse reflectance mode (R) were transformed to the Kubelka– Munk work F(R) to isolate the degree of light absorption from dispersing. The immediate band gap energies of Zr-ZnO catalysts was acquired from the plot of the

adjusted Kubelka– Munk work $[F(R)E]^{2.0}$ versus the energy of the absorbed light E are appeared in figure 6 The immediate band gap energy of Zr-ZnO particles is 3.02eV.

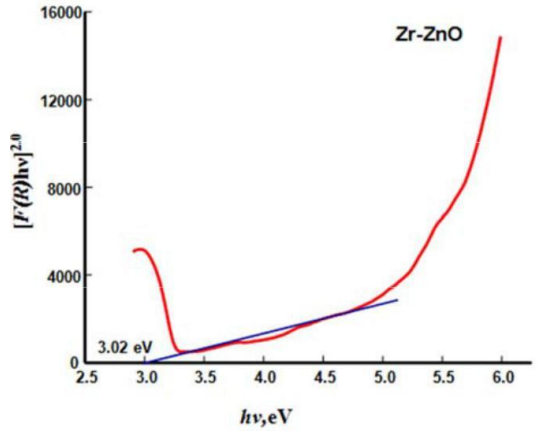

Figure 5. Tauc plot for direct band gap energy

■ ***Photoluminescence***

The photoluminescence (PL) spectra of the exposed ZnO and Zr– ZnO, are appeared in figure 6 and figure 7 separately. Photoluminescence happens because of the recombination of electron– hole pair in the semiconductor. The stacking Zr with ZnO does not shift the emission of ZnO, yet the power of PL emission diminishes when contrasted with uncovered ZnO. The catching of photogenerated electron by Zr lessens the electron– hole recombination prompting the abatement of PL emission. This lessening in the rate of electron– hole recombination improved the photocatalytic activity of ZnO.

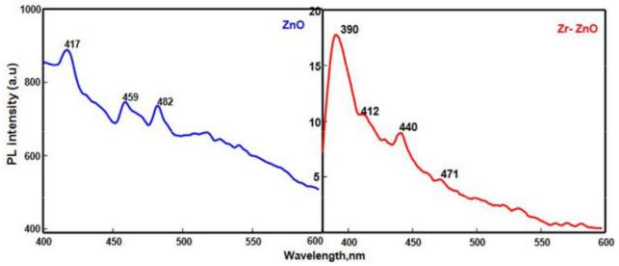

Figure 6. Photoluminescence spectra

■ ***Dye Degradation***

The fleeting profiles degradation of methylene blue dye under visible light is appeared in figure 6. It is noticed that the 58% (staying 4.5ppm dye solution) degradation is watched for Zr-ZnO in 180 min. while ZnOdegrade 41% (staying 6.2 ppm dye solution) in 180 min. This may be because of catching photo-energized electrons at conduction band by diminishing the electron-hole recombination as a result of Zr dopant into ZnO condition. Doping has managed the degradation happened by displaying the most elevated photo synergist degradation productivity in methylene blue dye This is on the grounds that the consolidated Zr molecule goes about as electron traps by stifling the recombination of photo-generated holes and electrons.

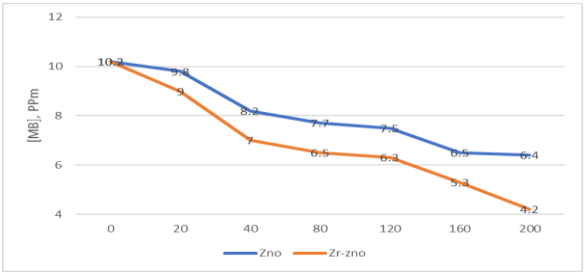

Figure 7. Temporal profiles of degradation of methylene blue dye under Visible light.

5. CONCLUSION

ZnO: Zr films demonstrated that doping offers command over resistivity decrease up to 4.8 at. % because of the additional particles offered by the substitution of Zr4+ to Zn2+. At heavier doping the carrier concentration was diminished because of Zr isolation to grain limits predictable with the concealment of grain development, and the formation of unbiased deformities at the limits (increment of zinc opportunities). The ≈ 2% Zr doped ZnO was set up by sol-gel method. XRD uncovers that readied Zr doped ZnO as hexagonal wurtzite structure and nonappearance of Zr^{3+}ion peak in ZnO crystals. SEM pictures demonstrates the readied doped ZnO micron in size and demolish the hexagonal wurtzite structure of ZnO with expansion of Zr^{3+} particle, EDX affirms the nearness of Zr^{3+} particle in ZnO crystals, DRS spectrum affirms the immediate band gap energy of Zr doped ZnO is 3.02eV. Zr^{3+} particle does not shift the emission of ZnO, yet the force of PL emission diminishes when contrasted with exposed ZnO. Zr doped ZnO is increasingly improved photocatalytic degradation of methylene blue dye than exposed ZnO under visible light.

6. REFERENCES

1. M. C. Uribe López, (2019). "Synthesis and Characterization of ZnO-ZrO_2Nanocomposites for Photocatalytic Degradation and Mineralization of Phenol", Journal of Nanomaterials Volume 2019, Article ID 1015876, 12 pages https://doi.org/10.1155/2019/1015876

2. Parangusan H (2018). "Nanoflower-like Yttrium-doped ZnO Photocatalyst for the Degradation of Methylene Blue Dye", Photochem Photobiol. 2018 Mar;94(2):237-246. doi: 10.1111/php.12867. Epub 2018 Jan 19.

3. Jun Song, (2017). "Soft Zr-doped TiO_2 Nanofibrous Membranes with Enhanced Photocatalytic Activity for Water

Purification", *Scientific Reports*volume 7, Article number: 1636 (2017)

4. S. M. Lama., J. A. Queka., J. C. Sin. Mechanistic investigation of visible light responsive Ag/ZnO micro/ nanoflowers for enhanced photocatalytic performance and antibacterial activity, J. of Photochem. Photobiol., A: Chem., vol. 353, pp. 171–184, 2018.

5. O. Bechambi., M. Chalbi., W. Najjara. and S. Sayadi (2015). Photocatalytic activity of ZnO doped with Ag on the degradation of endocrine disrupting under UV irradiation and the investigation of its antibacterial activity, applied surface science, http://dx.doi.org/doi:10.1016/j.apsusc.2015.03.049.

6. S. N. Basahel., Tarek T Ali, M. Mokhtar and K. Narasimharao : Influence of crystal structure of nanosized ZrO_2 on photocatalytic degradation of methyl orange, Nano. Res. Lett., DOI 10.1186/s11671-015-0780-z.

7. N. C. S. Selvam., J. J. Vijaya., L. J. Kennedy (2012). Effects of Morphology and Zr Doping on Structural, Optical, and Photocatalytic Properties of ZnO Nanostructures, Ind. Eng. Chem. Res. Vol. 51, pp. 16333.

8. F. G. Wang., M. S. Lv., Z. Y. Pang., T. L. Yang., Y. Dai., S. H. Han (2008). Theoretical study of structural, optical and electrical properties of zirconium-doped zinc oxide, Appl. Surf. Sci. vol. 254, pp. 6983.

9. Q. Hou. C. Zhao., Z. Xu (2016). Effect of Zr doping on the electrical and optical properties of ZnO, Chem Phys. Lett., http://dx.doi.org/10.1016/j.cplett.2016.06.075 .

10. Kapusuz, D., J. Park and A. Ozturk (2013). Sol–gel synthesis and photocatalytic activity of B and Zr–doped TiO2 Journal of Physics and Chemistry of Solids 74: pp. 1026–1031.

11. Matejova, L., K. Koci, M. Reli, L. Capek, V. Matejka, O. Solcova and L. Obalova (2013). On sol–gel derived Au-enriched TiO2 and TiO2-ZrO2 photocatalysts and their investigation in photocatalytic reduction of carbon dioxide Applied Surface Science 285: pp. 688– 696.

12. Kokporka, L., S. Onsuratoom, T. Puangpetch and S. Chavadej (2013). Sol–gel synthesized mesoporous assembled TiO2–ZrO2 mixed oxide nano crystals and their photocatalytic sensitized H2 production activity under visible light irradiation Materials Science in Semiconductor Processing 16: pp. 667–678.

13. C. Y. Tsay., K. S. Fan (2008). Optimization of Zr-doped ZnO thin films prepared by sol-gel method, Mater. Trans., vol. 49, pp. 1900.

14. Lin, M.; Chang, Y.; Chen, M.; Chu, C. (2011). Characteristics of Zr-doped ZnO thin films grown by atomic layer deposition. J. Electrochem. Soc. 2011, 158, pp. D395–D399

15. Kambur., G. S Pozan., I. Boz (2012). Preparation, characterization and photocatalytic activity of TiO_2–ZrO_2 binary oxide nanoparticles, Appl. Catal. B: Environ. vol. 115, pp. 149–158.

16. J. C. Tristao., F. Magalhaes., P. Corio. M. T. C. Sansiviero (2006). Electronic characterization and photocatalytic properties of CdS/TiO_2 semiconductor composite, J. Photochem. Photobiol. A: Chem., vol. 181, pp. 152–157.

17. K. Vignesh., R. Priyanka., M. Rajarajan. A. Suganthi (2013). Photo reduction of Cr (VI) in water using Bi_2O_3–ZrO_2 nanocomposite under visible light irradiation, Mater. Sci. Eng. B, vol. 178, pp. 149–157.

18. W. Zheng. Z. Bingru. L. I. Fengting (2007). A simple and cheap method for preparation of coupled ZrO_2/ZnO with high photocatalytic activities, Front. Environ. Sci. Eng. China. vol 1, pp. 454–458.

19. E. D, Sherly. J. Judith Vijaya. N. Clament Sagaya Selvam. L. John Kennedy (2014). Microwave assisted combustion synthesis of coupled ZnO–ZrO_2 nanoparticles and their role in the photocatalytic degradation of 2, 4-dichlorophenol, Ceram. Inter., vol. 40, pp. 5681–5691.

Corresponding Author

Pooja*

Extension Lecturer of Chemistry, Govt. College, Israna, Panipat

poojajaglan007@gmail.com